

# Inclusion Effect and Structural Basis of Cyclodextrins for Increased Extraction of Medicinal Alkaloids from Natural Medicines

Miyoko KAMIGAUCHI,<sup>\*,a</sup> Kazuko KAWANISHI,<sup>a</sup> Hirofumi OHISHI,<sup>b</sup> and Toshimasa ISHIDA<sup>b</sup>

<sup>a</sup> Kobe Pharmaceutical University; Motoyama Kitamachi, Higashinada-ku, Kobe 658–8558, Japan: and <sup>b</sup> Osaka University of Pharmaceutical Sciences; Nasahara, Takatsuki, Osaka 569–1094, Japan.

Received May 23, 2006; accepted February 6, 2007

The enhancing effects of  $\alpha$ -,  $\beta$ -, and  $\gamma$ -cyclodextrins (CyDs) on the aqueous extraction of ephedrine and berberine from the natural medicines were investigated in HPLC analysis, and the greatest effect was observed for  $\beta$ - and  $\gamma$ -CyDs. To clarify the structural basis of such an increased extraction effect with  $\beta$ -CyD, possible interaction modes of (1*R*,2*S*)-ephedrine with  $\alpha$ -,  $\beta$ -, and  $\gamma$ -CyDs were investigated using molecular dynamic simulations in an aqueous solution system. It was shown that the wrapping model of ephedrine by  $\beta$ -CyD is the most compact and thus increases the solubility most effectively, compared with those by other CyDs. The same mode could be possible for the greatest effect of  $\gamma$ -CyD on the extraction of berberine from natural medicines. This clearly shows that CyDs are useful additives for the effective extraction of bioactive alkaloids from natural medicines.

**Key words** natural medicine; cyclodextrin; inclusion structure; alkaloid; molecular dynamic calculation; molecular orbital calculation

Natural materials such as Coptis Rhizome, Phellodendron Bark, and Ephedra Herb have been widely used as Chinese medicines. The main active components of these natural medicines are alkaloids such as berberine (1) and ephedrine (2) (Fig. 1). In the Japanese pharmacopoeia, a regulation value<sup>1)</sup> has been applied for the alkaloid contents in these natural medicines; the alkaloid content for drug efficacy should be  $\geq 4.2\%$  in Coptis Rhizome,  $\geq 1.2\%$  in Phellodendron Bark, and  $\geq 0.7\%$  in Ephedra Herb. However, the alkaloid content in the plants differs depending on the locality and climate conditions. Furthermore, the alkaloid content may decrease due to technical problems during the extraction process. Therefore it is important for the manufacturer to maintain the standard value of the alkaloid content in the extracted liquid.

Generally, the solubility of alkaloids with an aromatic ring is relatively poor in water due to its large hydrophobicity. In this case, it could be expected that a hydrophilic annular molecule would increase the solubility, because of the inclusion effect for the alkaloid. Cyclodextrin (CyD) has been recog-

nized as an effective additive in the actual usage of pharmaceuticals. CyD is a family of cyclic oligosaccharides consisting of six ( $\alpha$ -CyD), seven ( $\beta$ -CyD), or eight ( $\gamma$ -CyD) glucose backbones (Fig. 1). As these CyDs show similar hydrophobic properties, the potential of increasing the solubility of a guest molecule depends on the compactness of the host–guest complex: the diameters of the inclusion cavities of  $\alpha$ -,  $\beta$ -, and  $\gamma$ -CyDs are *ca.* 4.5 Å, 7.0 Å, and 8.5 Å, respectively.<sup>2–8)</sup>

In a previous paper,<sup>9)</sup> we analyzed possible interaction modes of berberine with  $\alpha$ -,  $\beta$ -, and  $\gamma$ -CyDs in an aqueous solution using NMR spectroscopy and molecular dynamic (MD) simulation and clarified that  $\gamma$ -CyD can form the most preferred inclusion complex with berberine. This result suggests the availability of  $\gamma$ -CyD for the effective extraction of berberine from natural medicines. To confirm this possibility, we examined the increasing effects of three types of CyDs on the extraction of berberine and ephedrine from natural medicines using HPLC. We also investigated possible interaction modes of (1*R*,2*S*)-ephedrine with these CyDs in an aqueous solution with MD simulation and molecular orbital (MO) methods.

## Experimental

**Materials** The dried and cut or powdered natural medicines, Coptis Rhizome [*Coptis japonica*, *Coptis chinensis*, *Coptis deltoide*, and *Coptis teeta* (Ranunculaceae)], Phellodendron Bark [*Phellodendron amurense* and *Phellodendron chinense* (Rutaceae)], Calumba Radix [*Columba jateorhiza* (Menispermaceae)], and Ephedra Herb [*Ephedra sinica*, *Ephedra intermedia*, and *Ephedra equisetina* (Ephedraceae)], were purchased from Tochimotoenkaido Co. (Japan). Cyclodextrins ( $\alpha$ -,  $\beta$ -, and  $\gamma$ -CyDs) were purchased from Nacalai Tesque Co. (Japan) and used after recrystallization from an aqueous solution.

**HPLC Measurement**  $\alpha$ -,  $\beta$ -, or  $\gamma$ -CyD (250 mg) was added to the test tube containing the material (1 g) in water (20 ml) and heated at 95 °C for 0.5 h in a metal bath. The extract was cooled at 24 °C while standing for 1 h, and the supernatant was filtered using a Millex-HA filter (Millipore Co.). The alkaloid content in the filtrate was measured using HPLC. HPLC was carried out on a Gilson HPLC system [pump, 306; detector, UV/VIS-151; column, Cosmosil 5C18-AR, 4.6 mm i.d.  $\times$  150 cm (Nacalai Tesque)]. Detection conditions of berberine were: mobile phase, H<sub>2</sub>O–MeCN–KH<sub>2</sub>PO<sub>4</sub>–SLS (250 ml:250 ml:1.7 g:0.85 g); flow rate, 0.9 ml/min; and UV detector, 345 nm. Detection conditions of ephedrine were: mobile phase, H<sub>2</sub>O–MeCN–HPO<sub>4</sub>–SLS (150 ml:10 ml:0.14 g:0.7 g); flow rate, 0.5 ml/min for

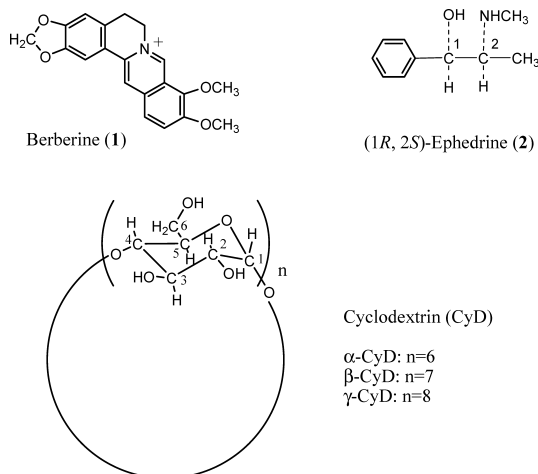


Fig. 1. Chemical Structures of Berberine (1), (1*R*,2*S*)-Ephedrine (2), and Cyclodextrins (CyD)

\* To whom correspondence should be addressed. e-mail: kamigami@kobepharm-u.ac.jp

0 to 10 min and 0.7 ml/min for 10 to 20 min; and UV detector, 254 nm.

**MD Simulation** The atomic coordinates of  $\alpha$ - and  $\beta$ -CyDs used for the MD calculations were constructed from their X-ray crystal analyses,<sup>10,11)</sup> and those of  $\gamma$ -CyD and (1*R*,2*S*)-ephedrine were constructed using Insight II/Discover 2000.<sup>12)</sup> The starting structures for the MD simulations were considered for the following four cases (Fig. 2), *i.e.*, the side chain or benzene ring moiety of ephedrine approaches from the side of the primary hydroxyl group (type 1 or type 2) or from the side of the secondary hydroxyl group of CyD (type 3 or type 4), respectively. Thus the MD simulations were performed for 12 cases [four types  $\times$   $\alpha/\beta/\gamma$ -CyD] in the aqueous solution system, where water molecules were added in the 6.0 Å-truncated octahedron cell shape. The CHARMM<sup>13)</sup> in Discovery Studio Modeling<sup>12)</sup> program package was used for the simulations, where the force field from cff<sup>14)</sup> was used and the time step of 1 fs was taken for the simulation. The cut-off radius was 13.5 Å in the group base, and the simulation was continued for 1 ns. By setting the periodic boundary conditions with an NVT ensemble, the MD simulations were performed, without modifications to the program code. The final temperature was set at 300 K.

The total energy value (kcal/mol) of the starting point (0 ps) and of the local minimum points at the MD simulation time (ps) from the MD calculation; type 1 of  $\alpha$ -CyD and ephedrine with 558H<sub>2</sub>O as solvent molecules in the MD cell: -3709.04 (0 ps), -3859.49 (143 ps). Type 2 of  $\alpha$ -CyD and ephedrine with 501H<sub>2</sub>O: -3374.98 (0 ps), -3472.83 (166 ps). Type 3 of  $\alpha$ -CyD and ephedrine with 371H<sub>2</sub>O: -2499.84 (0 ps), -2528.87 (474 ps). Type 4 of  $\alpha$ -CyD and ephedrine with 424H<sub>2</sub>O: -2873.11 (0 ps), -2939.22 (420 ps). Type 1 of  $\beta$ -CyD and ephedrine with 640H<sub>2</sub>O: -4354.11 (0 ps), -4461.42 (144 ps). Type 2 of  $\beta$ -CyD and ephedrine with 547H<sub>2</sub>O: -3620.10 (0 ps), -3773.26 (220 ps). Type 3 of  $\beta$ -CyD and ephedrine with 428H<sub>2</sub>O: -2769.52 (0 ps), -2854.34 (72.8 ps), and -2845.43 (524.8 ps). Type 4 of  $\beta$ -CyD and ephedrine with 533H<sub>2</sub>O: -3537.70 (0 ps), -3730.61 (488 ps), and -3728.26 (825.6 ps). Type 1 of  $\gamma$ -CyD and ephedrine with 773H<sub>2</sub>O: -5240.67 (0 ps), -5344.85 (465 ps). Type 2 of  $\gamma$ -CyD and ephedrine with 635H<sub>2</sub>O: -4375.22 (0 ps), -4417.01 (220 ps). Type 3 of  $\gamma$ -CyD and ephedrine with 554H<sub>2</sub>O: -3704.99 (0 ps), -3809.31 (372 ps). Type 4 of  $\gamma$ -CyD and ephedrine with 561H<sub>2</sub>O: -3743.01 (0 ps), -3852.74 (443 ps).

**MO Calculation** Because the numbers of water molecules included in the respective calculation systems are different depending on the starting structures of MD simulations, the heat of formation for the respective MD-simulated molecular complexes (excluding water molecules) were calculated

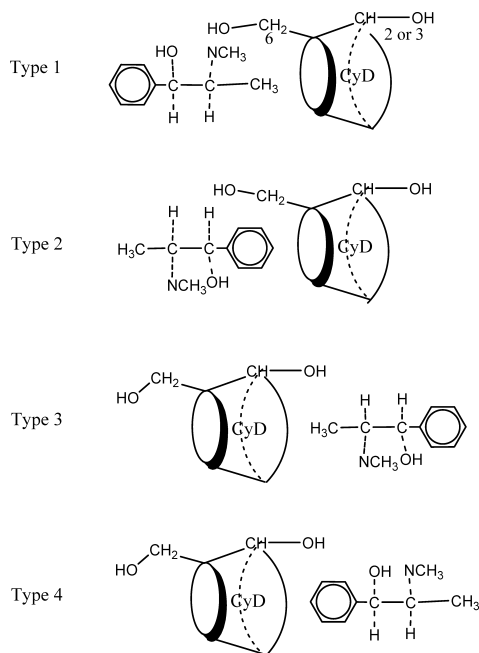


Fig. 2. Four Different Starting Structures (Types 1–4) for MD Simulation of Ephedrine–CyD Interaction

Type 1 or type 2: the side chain or benzene ring moiety of ephedrine approaches from the primary hydroxyl C(6)-OH group side of CyD; type 3 or type 4: the side chain or benzene ring moiety of ephedrine approaches from the secondary hydroxyl group (C(2)-OH and C(3)-OH) side of CyD.

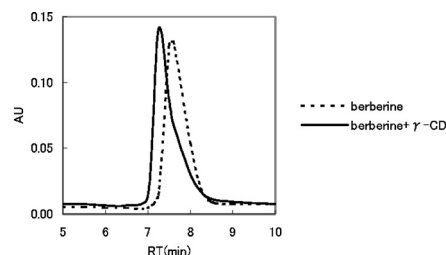
using the MO method with the MOPAC Var. 6<sup>15)</sup> in the MOL/MOLIS<sup>16)</sup> system, to compare their energetic stabilities. The complexes were calculated once (1 SCF) using the PM3 Hamiltonian.

The heat of formation (kcal/mol) of type 1 of  $\beta$ -CyD and ephedrine of the local minimum points at the MD simulation time (ps): -1221.39 kcal/mol (144 ps). Type 2 of  $\beta$ -CyD and ephedrine: -1220.69 kcal/mol (220 ps). Type 3 of  $\beta$ -CyD and ephedrine: -1243.51 kcal/mol (72.8 ps) and -1230.41 kcal/mol (524.8 ps). Type 4 of  $\beta$ -CyD and ephedrine: -1241.40 kcal/mol (488 ps) and -1241.32 kcal/mol (825.6 ps).

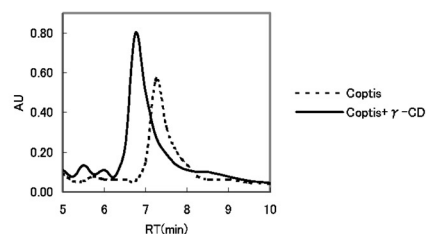
Table 1. Effect of CyD Addition on Alkaloid Extraction by HPLC

Material	Added CyD	Increasing rate relative to CyD-free (%)
Ephedra Herb	Cut	$\alpha$ -CyD 109 (ephedrine)
Ephedra Herb	Cut	$\beta$ -CyD 135 (ephedrine)
Ephedra Herb	Cut	$\gamma$ -CyD 112 (ephedrine)
Coptis Rhizome	Powder	$\alpha$ -CyD 118 (berberine)
Coptis Rhizome	Powder	$\beta$ -CyD 124 (berberine)
Coptis Rhizome	Powder	$\gamma$ -CyD 133 (berberine)
Phellodendron Bark	Powder	$\alpha$ -CyD 111 (berberine)
Phellodendron Bark	Powder	$\beta$ -CyD 123 (berberine)
Phellodendron Bark	Powder	$\gamma$ -CyD 143 (berberine)
Calumba	Powder	$\alpha$ -CyD 102 (berberine)
Calumba	Powder	$\beta$ -CyD 112 (berberine)
Calumba	Powder	$\gamma$ -CyD 118 (berberine)

a) Berberine



b) Berberine in *Coptis Rhizome*



c) Ephedrine in *Ephedra Herb*

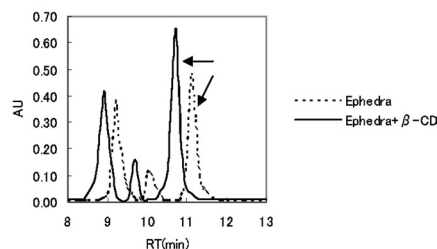


Fig. 3. HPLC Profiles of Berberine (a and b) and Ephedrine (c)

(a) Standard berberine (dotted line) and its berberine+ $\gamma$ -CyD (1 g/l) (solid line); (b) extracted berberine in *Coptis Rhizome* (dotted line) and *Coptis Rhizome*+ $\gamma$ -CyD (60 g/l) (solid line); (c) extracted ephedrine in *Ephedra Herb* (dotted line) and *Ephedra Herb*+ $\beta$ -CyD (60 g/l) (solid line). The arrows in Fig. 3(c) represent the elution position of ephedrine.

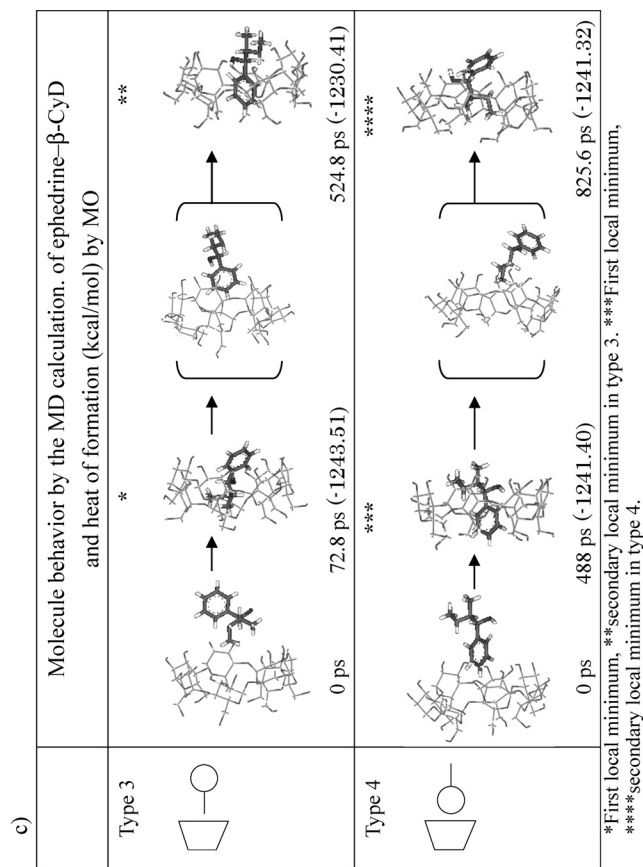
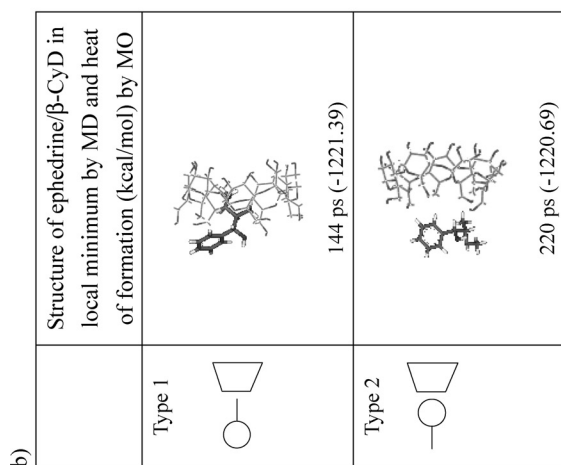
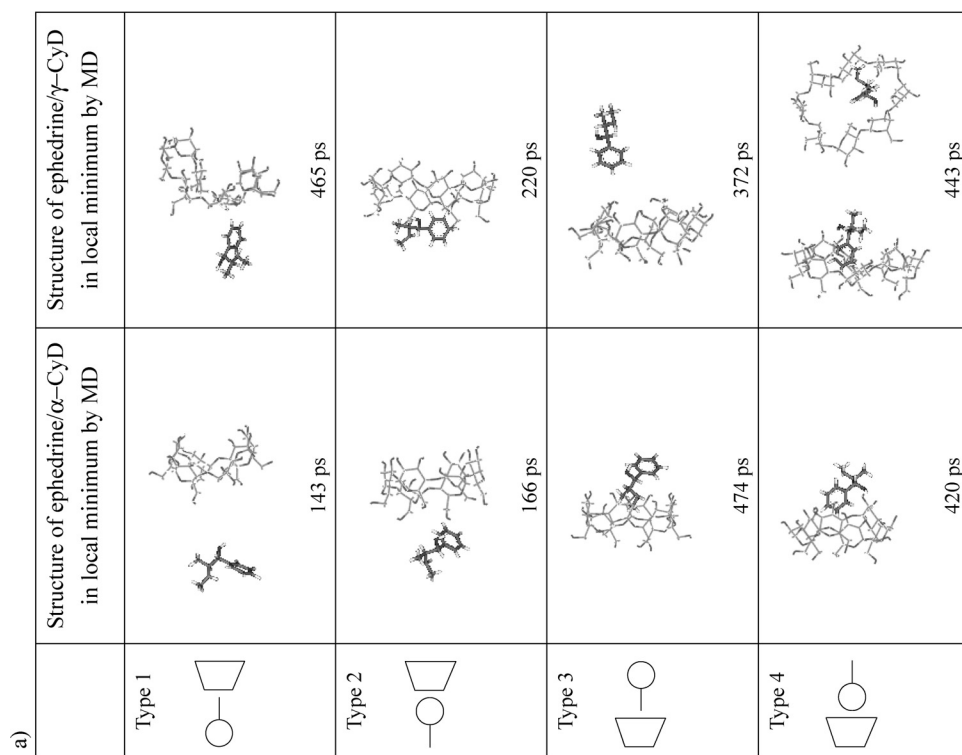


Fig. 4. The Snapshot of (1*R*,2*S*)-Ephedrine-CyD Complex of the Lowest Negative Total Energy during MD Simulation of 1000 ps in Types 1—4

a) Ephedrine- $\alpha$ - (left side) and  $\gamma$ -CyD (right side) complexes of types 1—4, where the ephedrine- $\gamma$ -CyD complex of type 4 is shown with two different views; b) ephedrine- $\beta$ -CyD complexes of types 1 and 2; c) MD simulation trajectory from the starting structure (0 ps) to two stable ephedrine- $\beta$ -CyD complexes taking nearly the same total energy in types 3 and 4. The MD parameters of respective complexes are given in Experimental.

## Results and Discussion

**Enhancing Effect of CyDs on Extraction of Berberine and Ephedrine from Natural Medicines** The effects of CyDs on the aqueous extraction of berberine and ephedrine from their natural medicines are shown in Table 1. The results showed that the extracted contents of berberine and ephedrine were clearly increased by the addition of CyD regardless of the type of CyD. The enhancing effect of CyD on the extraction of berberine was in the order of  $\gamma$ -> $\beta$ -> $\alpha$ -CyD in all three materials, Coptis Rhizome, Phellodendron Bark, and Calumba Radix. The HPLC elution profile for the extraction of berberine from Coptis Rhizome (powder) is shown in Fig. 3. The peak of  $\gamma$ -CyD-added standard berberine (Fig. 3a, solid line) was little changed as compared with that of  $\gamma$ -CyD-free berberine (Fig. 3a, dotted line), although a slight change was observed in the shape and retention time. In contrast, the addition of  $\gamma$ -CyD to the natural medicines increased the extraction content of berberine considerably (Fig. 3b). This agrees well with our previous paper,<sup>9)</sup> in which we reported that berberine interacts best with  $\gamma$ -CyD among the three types of CyDs in an aqueous solution and this leads to the enhanced solubility of berberine in water. Thus the present results appear to reflect that the ranking order for the extraction effect corresponds to the binding fitness of berberine to CyD, and the molecular structure and size of berberine are the most suitable for the inclusion complex formation with  $\gamma$ -CyD.

On the other hand, ephedrine, a major component of Ephedra Herb, belongs to a phenethylamine group and has been used as a cough medicine and expectorant. By the addition of three CyDs, an increase of 9–35% was observed for the extraction of ephedrine from Ephedra Herb (cut) (Table 1). In contrast to the case of berberine, the content of ephedrine was increased in the order of  $\beta$ -> $\gamma$ -> $\alpha$ -CyD; the  $\beta$ -CyD preferential increase in ephedrine extracted is shown in Fig. 3c. Because the molecular size of ephedrine is smaller than that of berberine, the interaction with  $\beta$ -CyD would be the most suitable.

### MD Simulation of (1R,2S)-Ephedrine–CyD Complex

Although spectroscopic study of the interaction between  $\beta$ -CyD and ephedrine has been reported,<sup>17)</sup> there is no report on the structure of the inclusion complex. Therefore MD simulations were performed to investigate the relationship between the interaction modes of ephedrine with  $\alpha$ -,  $\beta$ -, and  $\gamma$ -CyDs and their enhancing effects on extraction. The process from the starting structure of ephedrine–CyD complex to its equilibrium state in an aqueous solution was simulated using MD calculations during 1000 ps. Four starting sets (types 1–4 in Fig. 2) were considered for  $\alpha$ -,  $\beta$ -, and  $\gamma$ -CyDs. The snapshots of the lowest negative total energies in complexes of types 1–4 are shown in Fig. 4.

In the interaction with  $\alpha$ - or  $\gamma$ -CyD, the ephedrine molecule was located near the side of the primary or secondary hydroxyl group of CyD (Fig. 4a), and this would result from the cavity size of  $\alpha$ - or  $\gamma$ -CyD being too small or too large to wrap the molecular size of ephedrine tightly, respectively; an exception was observed for the structure of the inclusion complex of the type 4 ephedrine– $\gamma$ -CyD (Fig. 4a), although the inclusion cavity of the  $\gamma$ -CyD left a large space. A similar tendency was also observed for the ephedrine– $\beta$ -CyD complexes of types 1 and 2 (Fig. 4b). In contrast,  $\beta$ -CyD

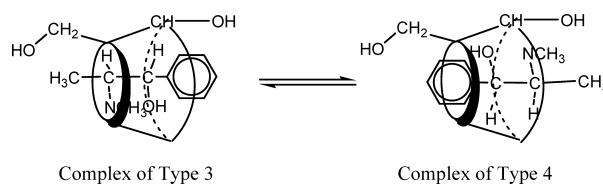


Fig. 5. Equilibrium Scheme of Two Stable Ephedrine– $\beta$ -CyD Complexes

formed a much more compact inclusion complex with ephedrine in type 3 or 4 (Fig. 4c), in which ephedrine was almost completely inserted into the inside cavity. It is interesting to note that when ephedrine approaches the side of secondary hydroxyl group of  $\beta$ -CyD, two nearly identical stable inclusion complexes are formed regardless of the molecular orientation of ephedrine. The energies (heat of formation) of these two complexes in the MO calculations are in the range of –1230––1244 kcal/mol (Fig. 4c) and are more stable than –1221 kcal/mol of types 1 and 2. This means that ephedrine is preferentially captured by  $\beta$ -CyD with an equilibrium state between the complex type 3 and complex type 4, as shown in Fig. 5.

The snapshots of ephedrine– $\beta$ -CyD complexes of type 3 at 72.8 ps and of type 4 at 488 ps are shown in Fig. 6. The  $\beta$ -CyD molecule wraps the fuselage of ephedrine so as to be fully inserted into the cavity of  $\beta$ -CyD. Although the N...O and O...O atomic pairs are beyond the hydrogen-bonding distance, they would contribute to the fixation of ephedrine into the cavity of  $\beta$ -CyD through the dynamic electrostatic interactions including hydrogen bonds during MD simulation. This mode of interaction can explain the enhancing effect of  $\beta$ -CyD on ephedrine from Ephedra Herb due to increasing the solubility of ephedrine in water, because the glucose molecules in  $\beta$ -CyD fully cover the hydrophobic benzene ring of ephedrine and consequently dissolve the inclusion complex through hydrogen bond formations between the glucose and water molecules.

In conclusion, the present study showed that i) CyDs increase the extraction contents of berberine and ephedrine from their natural materials due to their increasing solubility in water; and ii) the efficiency for the extraction is closely related to the formation of the stable inclusion complex, which is dependent on the combination of the molecular size and shape of the guest molecule with the inside cavity size of CyD, i.e.,  $\beta$ -CyD for ephedrine and  $\gamma$ -CyD for berberine. The present results indicate the usefulness of CyDs as powerful additives for increasing the extraction content of bioactive components from natural material.

## References

- 1) The Japanese Pharmacopoeia, 14th ed., Yakuji Nippo, Tokyo, 2001, pp. 823–825, 861, 975.
- 2) Uekama K., *Yakugaku Zasshi*, **124**, 909–935 (2004).
- 3) Chen W. H., Hayashi S., Tahara T., Nogami Y., Koga T., Yamaguchi M., Fujita K., *Chem. Pharm. Bull.*, **47**, 588–589 (1999).
- 4) Breslow R., Dong S. D., *Chem. Rev.*, **98**, 1997–2011 (1998).
- 5) Loftsson T., Brewster M., *J. Pharm. Sci.*, **85**, 1017–1025 (1996).
- 6) Wenz G., *Angew. Chem.*, **106**, 851–870 (1994).
- 7) Szejtli J., “Cyclodextrins and Their Inclusion Complexes,” Akadémiai Kiadó, Budapest, 1982.
- 8) Irie T., Otagiri M., Sunanda M., Uekama K., Ohtani Y., Sugiyama Y., *J. Pharmacobio-Dyn.*, **5**, 741–744 (1982).
- 9) Kamiguchi M., Kanbara N., Sugiura M., Iwasa K., Ohishi H., Ishida T., *Helv. Chim. Acta*, **87**, 264–271 (2004).



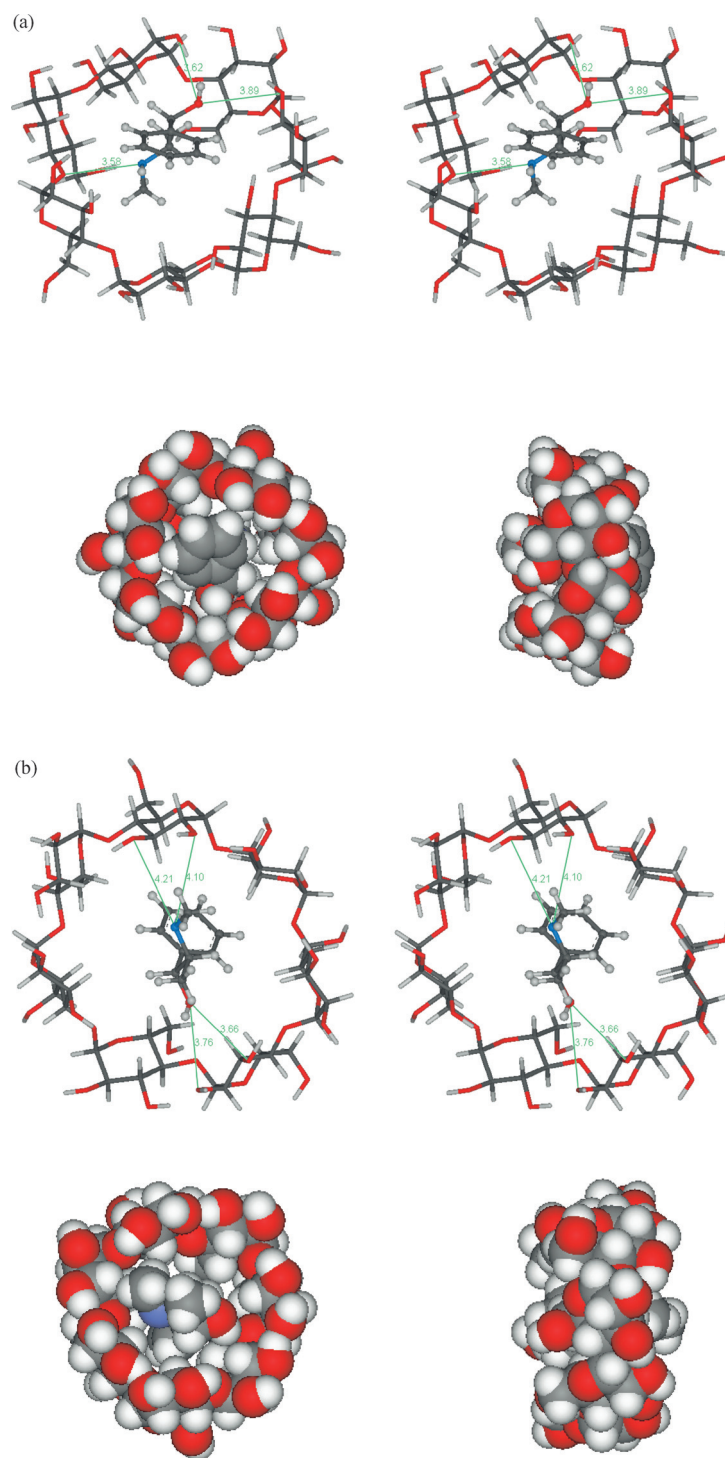


Fig. 6. Stereoscopic Views of Snapshots (Ephedrine: Ball and Stick Model,  $\beta$ -CyD: Stick Model) of Ephedrine- $\beta$ -CyD Complexes of Type 3 at 72.8 ps (a) and Type 4 at 488 ps (b)

CPK models of these complexes are shown from two different views on the lower side. The selected N $\cdots$ O and O $\cdots$ O atomic pairs between ephedrine and  $\beta$ -CyD are shown by green lines, together with their interatomic distances (Å). In CPK models, the front and side views from the secondary hydroxyl group side of  $\beta$ -CyD are shown on the left and right sides, respectively.

- 10) Lindner K., Saenger W., *Acta Cryst. Sect. B, Struct. Crystallogr. Cryst. Chem.*, **38**, 203—210 (1982).
- 11) Steiner T., Koellner G., *J. Am. Chem. Soc.*, **116**, 5122—5128 (1994).
- 12) Accelrys Software Inc., San Diego, CA, U.S.A.
- 13) Momany F. A., Rone R., *J. Comp. Chem.*, **13**, 888—900 (1992).
- 14) Hwang M. J., Stockfisch T. P., Hagler A. T., *J. Am. Chem. Soc.*, **116**, 2515—2525 (1994).
- 15) Stewart J. J. P., *J. Comput. Chem.*, **10**, 221—264 (1989).
- 16) “Molecular Orbital Analysis System,” Daikin Industries, Ltd., Japan, 1996
- 17) Ndou T. T., Mukundan S., Jr., Warner I. M., *J. Incl. Phenom. Mol. Recogn. Chem.*, **15**, 9—25 (1993).